4 Physicochemical and biological characterization of targeted, nucleic acid-containing nanoparticles[†]

4.1 Abstract

Nucleic acid-based therapeutics have the potential to provide potent and highly specific treatments for a variety of human ailments. However, systemic delivery continues to be a significant hurdle to success. Multifunctional nanoparticles are being investigated as systemic, nonviral delivery systems, and here we describe the physicochemical and biological characterization of cyclodextrin-containing polycations (CDP) and their nanoparticles formed with nucleic acids including plasmid DNA (pDNA) and small interfering RNA (siRNA). These polycation/nucleic acid complexes can be tuned by formulation conditions to yield nanoparticles with sizes ranging from 60-150 nm, zeta potentials from 10-30 mV, and molecular weights from ~$7x10^7$-$1x10^9$ g mol^{-1} as determined by light scattering techniques. Inclusion complexes formed between adamantane (AD)-containing molecules and the β-cyclodextrin molecules enable the modular attachment of polyethylene glycol (AD-PEG) conjugates for steric stabilization and targeting ligands (AD-PEG-transferrin) for cell-specific targeting. A 70-nm nanoparticle can contain ~10,000 CDP polymer chains, ~2,000 siRNA molecules, ~4,000 AD-PEG_{5000} molecules, and ~100 AD-PEG_{5000}-Tf molecules; this represents a significant payload of siRNA and a large ratio of siRNA to targeting ligand (20:1). The nanoparticles protect the nucleic acid payload from nuclease degradation, do not

[†] Reproduced with permission from: Bartlett, D.W. and Davis, M.E. (2007) Physicochemical and biological characterization of targeted, nucleic acid-containing nanoparticles. *Bioconjugate Chem*, **18,** 456-468. Copyright 2007 American Chemical Society.

aggregate at physiological salt concentrations, and cause minimal erythrocyte aggregation and complement fixation at the concentrations typically used for in vivo application. Uptake of the nucleic acid-containing nanoparticles by HeLa cells is measured by flow cytometry and visualized by confocal microscopy. Competitive uptake experiments show that the transferrin-targeted nanoparticles display enhanced affinity for the transferrin receptor through avidity effects (multi-ligand binding). Functional efficacy of the delivered pDNA and siRNA is demonstrated through luciferase reporter protein expression and knockdown, respectively. The analysis of the CDP delivery vehicle provides insights that can be applied to the design of targeted nucleic acid delivery vehicles in general.

4.2 Introduction

Nucleic acid-based therapeutics are envisioned to play a significant role in the next generation of treatments for a variety of diseases such as cancer. In addition to the classic gene therapy approach of delivering DNA to replace mutated or absent genes, nucleic acid molecules can also be used to regulate the production of disease-associated proteins at both the transcriptional and translational levels. These nucleic acid-based drugs have received significant attention as promising new therapeutics, yet their application in vivo has been largely limited by the challenge of delivery; this has been particularly true for systemic delivery.

Naked nucleic acid molecules are rapidly degraded by ubiquitous nucleases present in the bloodstream. Double-stranded nucleic acid molecules ranging in size from small-interfering RNAs (siRNAs) to plasmids (pDNA) have a half-life of less than one hour in serum (1-3). Selective chemical modification of nucleic acids can increase

nuclease resistance and enable systemic delivery of naked siRNA molecules with functional efficacy in vivo (1,4). However, even nuclease-stabilized nucleic acids must still overcome other elimination barriers such as renal clearance that severely limit the efficacy of systemically delivered, small nucleic acid therapeutics (5). Attachment of specific targeting ligands can induce binding to protein carriers or uptake by the desired population of cells to be treated. Bioconjugates of the nucleic acid therapeutics covalently attached directly to targeting ligands such as cholesterol and antibodies have shown efficacy both in vitro and in vivo (4,6). While these methods for nuclease stabilization and covalent attachment of targeting ligands are promising for small nucleic acid therapeutics, the use of lipid- or polymer-based delivery vehicles is an approach for systemic delivery that can provide functions not achievable with naked nucleic acids or their covalent attachment to targeting moieties.

Carrier-mediated delivery has several advantages over the delivery of individual nucleic acid molecules. Encapsulation of the payload within a lipid bilayer or through electrostatic interactions is nonspecific, so these delivery vehicles can be used for generalized nucleic acid delivery. The use of a carrier enables delivery of many nucleic acid molecules per uptake event (this is especially important if the uptake involves highly specific cell-surface receptors since they are typically low in number), and isolation from exposure to the systemic environment can permit the use of unmodified nucleic acids (7). Modularly designed delivery vehicles can also take advantage of covalent or non-covalent attachment of hydrophilic polymers for steric stabilization and/or targeting ligands for cell-specific delivery, two critical features for systemic delivery (7,8). Such

modifications can affect the resulting biodistribution of delivery vehicles through passive and/or active targeting (7-10).

Passive targeting occurs as a result of the intrinsic physicochemical properties of the delivery vehicle. For example, the charge and size of the delivery vehicle alone can bias its biodistribution. The charge of the delivery vehicle significantly impacts its interaction with components of the bloodstream; highly charged particles can lead to complement activation, while near-neutral particles exhibit reduced phagocytic uptake (11,12). Specifically, cationic polymers such as polylysine and polyethylenimine have been shown to activate the complement system, and increasing polycation length and surface charge density lead to higher complement activation (11). Rapid binding of charged molecules by complement proteins or other opsonins can lead to immune stimulation and rapid clearance of the delivery vehicles from the bloodstream. The size of the delivery vehicle also matters for systemic delivery. Based on measured sieving coefficients for the glomerular capillary wall, it is estimated that the threshold for first-pass elimination by the kidneys is approximately 10 nm (diameter) (13), placing a lower size limit on the assembled delivery vehicles. On the other end of the size spectrum, macromolecular complexes preferentially accumulate in tumors through the enhanced permeability and retention (EPR) effect. However, large macromolecules or delivery vehicles exhibit limited diffusion in the extracellular space, such as the tumor interstitium, and in the complex intracellular environment (14); in both situations, restricted movement will severely limit efficacy by preventing uptake by a sufficient number of cells or hindering the ability of the delivered nanoparticles to localize to intracellular compartments such as the nucleus. Other restrictions limiting the maximum

size of delivery vehicles can also be imposed by the selectivity of receptors on certain cell types. For example, a study by Rensen et al. demonstrated that nanoparticles larger than 70 nm in diameter were not recognized by the asialoglycoprotein receptor (ASGPR) (15), placing an upper size limit on the nanoparticles that can be delivered to hepatocytes through this receptor.

Recent efforts toward targeted delivery have focused on decorating the surface of delivery vehicles with cell surface receptor-specific targeting ligands as a means of active targeting. Hydrophilic polymers, such as polyethylene glycol (PEG), can be attached to the surface of the delivery vehicles to mask surface charge and prevent nonspecific interactions, helping to prevent unwanted binding to components of the bloodstream, slow uptake by the reticuloendothelial system (RES), and alter the cellular uptake patterns (8,16). Further addition of entities that can interact with cell surface receptors, such as the receptors' natural ligands, antibodies, or antibody fragments, allows the delivery vehicle to target particular cell types and undergo receptor-mediated endocytosis upon binding to the surface receptor (7,8,15).

In light of these considerations, a successful delivery vehicle must be engineered to have the following characteristics: (i) be small enough to extravasate and exhibit adequate tissue penetration, yet avoid rapid renal clearance; (ii) minimize nonspecific interactions and opsonization while providing specific targeting to a given cell; and (iii) protect the nucleic acid from degradation, but willingly release it upon arrival at the proper site. Over the past few years, we have been developing a synthetic delivery system based on a cyclodextrin-containing polycation (CDP) that has demonstrated some success in delivering nucleic acid payloads that include pDNA, siRNA, and DNAzymes

(7,17-20). This delivery system is the first to be *de novo* designed for systemic delivery of nucleic acids and completely formulated by self-assembly (17). Here, we describe the physicochemical and biological characterization of the cyclodextrin-containing polycation delivery system and its formulation with nucleic acids. We illustrate issues of importance when designing any polycation composite with nucleic acids through the use of the CDP and point out when the conclusions are specific to this system only.

4.3 Materials and methods

4.3.1 Formulation of nucleic acid nanoparticles

The chemical structure of the cyclodextrin-containing polycation is shown in Figure 4.1A. This short, linear polycation can be synthesized with (CDP-Im) or without (CDP) the imidazole groups on the terminal amines (17,18). A schematic showing nanoparticle formation using CDP-Im and nucleic acid is shown in Figure 4.1B; nanoparticles are formed by mixing equal volumes of CDP-Im and nucleic acid. The ratio of positive (+) charges (2 moles of positive charge per CDP-Im monomer; denoted β-CD) to negative (-) charges (1 mole of negative charge per nucleotide) is defined as the formulation charge ratio (+/-). Polyethylene glycol (PEG) molecules containing adamantane (AD) on the proximal end and either methoxy (AD-PEG) or a targeting ligand such as transferrin (AD-PEG-Tf) on the distal end can be attached to the surface of the nanoparticles via inclusion complex formation between adamantane and the β-CD molecules on the polycation backbone (16,17). The molecular weight of the PEG chain is typically 5,000 daltons (PEG_{5000}).

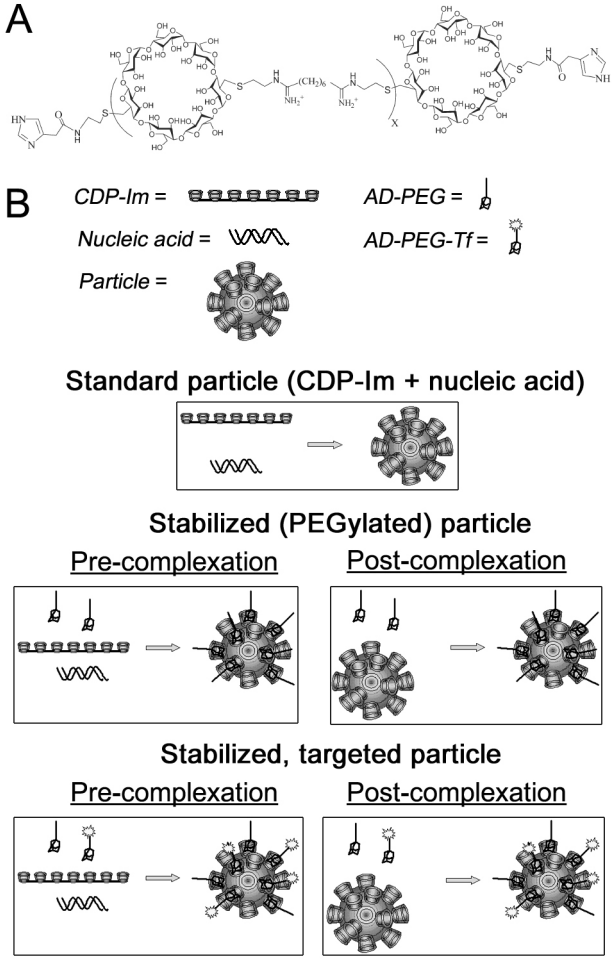

Figure 4.1. Formation of nucleic acid-containing nanoparticles using CDP-Im. (A) Schematic of the chemical structure of CDP-Im. (B) Schematic of nanoparticle assembly.

4.3.2 Formulation of PEGylated/targeted nucleic acid nanoparticles

Pre-complexation (self-assembly)

Before addition to the nucleic acid, the CDP or CDP-Im was mixed with an AD-PEG conjugate at a 1:1 AD-PEG:β-CD (mol:mol) ratio in water. Targeted nanoparticles also require the addition of ligand-modified AD-PEG-X (e.g., AD-PEG-Tf (7,19,20)) as a percentage of the total AD-PEG in the mixture. For example, 1 mol% AD-PEG-Tf nanoparticles contain 0.01 moles AD-PEG-Tf for every 0.99 moles AD-PEG. The mixture of CDP (or CDP-Im), AD-PEG, and AD-PEG-Ligand in water was then added to

an equal volume of nucleic acid in water such that the ratio of positive charges from CDP or CDP-Im to negative charges from the nucleic acid was equal to the desired charge ratio. A schematic of this assembly process is shown in Figure 4.1B. Unless specified otherwise, all PEGylated or targeted nucleic acid nanoparticles used in these studies were prepared through the pre-complexation method.

Post-complexation

Particles were initially formulated in water by mixing equal volumes of nucleic acid and the cyclodextrin-containing polycation. After nanoparticles had formed, the AD-PEG and AD-PEG-Tf conjugates were added directly to the formulation mixture at the desired ratio of AD-PEG:β-CD (mol:mol). A schematic of this assembly process is shown in Figure 4.1B.

4.3.3 Electrophoretic mobility shift assay

siRNA-containing nanoparticles were formulated at different charge ratios by changing the amount of CDP added to 1 μg of siRNA. CDP was first dissolved in 10 μL water and then added to an equal volume of water containing 1 μg of nucleic acid. After a 30-min incubation at room temperature, 10 μL of each formulation was run on a 1% agarose gel and visualized by ethidium bromide staining.

4.3.4 Individual nanoparticle charge ratio

siRNA nanoparticles were formulated in 40 μL water at charge ratios from 5 to 30 (+/-). After formulation, the nanoparticles were separated from the free components by addition of 400 μL PBS, to cause nanoparticle aggregation, followed by centrifugation to pellet the aggregated nanoparticles. Since the CDP is terminated by primary amines, quantitation of polycation content was accomplished by measuring the amount of primary

amines as follows. 400 μL of the supernatant was removed and combined with 200 μL of 0.01% w/v 2,4,6-trinitrobenzenesulfonic acid (Sigma). After incubating these samples for 2 h at 37°C, 200 μL 10% SDS and 100 μL of 1 N HCl were added to each sample before measuring the absorbance at 335 nm with a spectrophotometer. The amount of CDP in each sample was determined by comparison to a standard curve of CDP. The total positive charge present in each sample was calculated from the mass of CDP present using the fixed charge density of 0.0014 moles "+" per gram. This gave the number of unbound "+" charges present, so the number of bound "+" charges in the nanoparticles could be determined by subtracting the number unbound from the total "+" charges added during formulation. Assuming 100% incorporation of the nucleic acid into the nanoparticles at a formulation charge ratio of 3 (+/-) (based on the electrophoretic mobility shift assays; see Results), the ratio of CDP to nucleic acid within each nanoparticle is equal to the number of bound "+" charges divided by the total number of "-" charges from the nucleic acid.

4.3.5 Serum stability

Particles were formulated in water at a charge ratio of 3 (+/-) with an siRNA concentration of 0.05 g L^{-1}. 10 μL of 100% mouse serum (Sigma) were added to 10 μL of the nanoparticle formulation and subsequently incubated for 4 h at 37°C and 5% CO_2. 0.25 μg naked siRNA in 5 μL water were added to 5 μL of 100% mouse serum and also incubated for 4 h at 37°C and 5% CO_2. For comparison to the t = 4 h samples, identical amounts of naked siRNA or siRNA nanoparticles were exposed to 50% mouse serum immediately before gel loading (t = 0 h). 10 μL of each sample (containing 0.25 μg siRNA) were loaded per well of a 1% agarose gel. Displacement of the nucleic acid from

the nanoparticles was achieved by adding 1% sodium dodecyl sulfate (SDS) to the sample immediately prior to gel loading. Gel electrophoresis was performed by applying 100 V for 30 min, and the bands were visualized by ethidium bromide staining.

4.3.6 Dynamic light scattering (DLS)

Particle formulations were diluted to a volume of 1.4 mL, placed in a cuvette, and inserted into a ZetaPALS (Brookhaven Instruments Corporation) instrument to measure both the size and zeta potential. Reported effective hydrodynamic diameters represent the average values from a total of 5-10 runs of 30 seconds each, while zeta potentials represent the average of 10 runs each.

4.3.7 Transmission electron microscopy (TEM)

Particles containing CDP-Im and siRNA (0.1 g L^{-1}) and PEGylated nanoparticles containing CDP-Im, AD-PEG (1:1 AD-PEG:β-CD mole ratio), and siRNA (0.5 g L^{-1}) were formulated in water at a charge ratio of 3 (+/-). Samples were stained with 2% uranyl acetate and then examined with an EM201C electron microscope (Philips).

4.3.8 Atomic force microscopy (AFM)

Particles containing CDP-Im and siRNA (0.1 g L^{-1}) and PEGylated nanoparticles containing CDP-Im, AD-PEG (1:1 AD-PEG:β-CD mole ratio), and siRNA (0.5 g L^{-1}) were formulated in water at a charge ratio of 3 (+/-). 20 μL of each formulation solution were dropped on a freshly cleaved mica disc (Ted Pella, Inc.) and dried with pressurized air. Images were acquired with a Digital Instruments MultiMode AFM with a Nanoscope IV controller in tapping mode at a scan rate of 1 Hz using a BS Multi75 probe (BudgetSensors) with a resonant frequency of 75 kHz and a force constant of 3 N m^{-1}. Height images were flattened and processed for visualization with the derivative matrix

convolution filter using WSxM scanning probe microscopy software (Nanotec Electronica).

4.3.9 Isothermal titration calorimetry (ITC)

A MicroCal MCS titration calorimeter was used to investigate the thermodynamic properties of the interaction between AD-PEG conjugates and the β-cyclodextrin molecules on the CDP-Im backbone. CDP-Im (free or in nanoparticles) at 0.22 mM total β-CD in water was placed in the sample cell of the instrument. The reference cell contained water alone without CDP-Im. Small amounts of an AD-PEG stock solution at a concentration of 2.2 mM in water were titrated into the sample cell in 25 separate 10-μL increments. Titrations were performed at 30°C. The measured parameters were δn, the number of moles of ligand (AD-PEG) added to the sample cell, and q, the amount of heat released or absorbed. The Simplex algorithm in the Origin data analysis software was used to determine the following parameters: K, the equilibrium binding constant; n, the number of available binding sites; and ΔH, the change in enthalpy. A more in-depth description of the thermodynamic analysis applied to ITC is provided by Blandamer et al. (21).

4.3.10 Percentage of AD-PEG$_{5000}$ bound after formulation

The small molecule, lactose (Lac), was attached to the end of AD-PEG$_{5000}$ to enable quantification using the Amplex Red Galactose Oxidase Assay Kit (Molecular Probes). Nanoparticles were formulated in a total volume of 100 μL water by adding a 50 μL solution containing CDP-Im and AD-PEG$_{5000}$-Lac (1:1 mole ratio of AD-PEG$_{5000}$-Lac: β-CD) in water to a 50 μL solution of siRNA in water. Control formulations were

created by mixing CDP-Im and AD-PEG_{5000}-Lac without siRNA in 100 μL water. Nanoparticles and control formulations were filtered with Biomax (Millipore) centrifugal filtration devices with a 50 kDa MWCO to separate free and bound components. The Amplex Red Galactose Oxidase Assay Kit (Molecular Probes) was used to quantify the amount of AD-PEG_{5000}-Lac in the filtrate and retentate of all samples. Concentrations were determined by comparison to a standard curve of AD-PEG_{5000}-Lac. The percentage of AD-PEG_{5000}-Lac bound to the nanoparticles was determined by subtracting the fraction of recovered AD-PEG_{5000}-Lac in the filtrate of the nanoparticle samples from the fraction of recovered AD-PEG_{5000}-Lac in the filtrate of the control samples.

4.3.11 Percentage of AD-PEG_{5000}-Tf bound after formulation

Tf-targeted nanoparticles were formulated in a total volume of 100 μL water by adding a 50 μL solution of CDP-Im, AD-PEG_{5000}, and AD-PEG_{5000}-Tf (1:1 mole ratio of AD-PEG_{5000}-X:β-CD where AD-PEG_{5000}-X was composed of either 1 mol% or 5 mol% AD-PEG_{5000}-Tf and the remainder AD-PEG_{5000}) in water to a 50 μL solution of siRNA in water. Control formulations were created by mixing CDP-Im, AD-PEG_{5000}, and AD-PEG_{5000}-Tf without siRNA in 100 μL water. Nanoparticles and control formulations were filtered with Nanosep (Millipore) centrifugal filtration devices with a 300 kDa MWCO to separate free and bound components. Total protein content in the filtrate (unbound AD-PEG_{5000}-Tf) and retentate (bound AD-PEG_{5000}-Tf) was determined using the BioRad DC protein assay. The percentage of AD-PEG_{5000}-Tf bound to the nanoparticles was determined by subtracting the fraction of recovered AD-PEG_{5000}-Tf in the filtrate of the nanoparticle samples from the fraction of recovered AD-PEG_{5000}-Tf in the filtrate of the control samples.

4.3.12 Multi-angle light scattering (MALS)

Particle formulations were loaded into a 10-mL syringe connected to a syringe pump to control the flow rate into a Dawn EOS (Wyatt Technology) multi-angle light scattering instrument. The typical flow rate used was 1 mL min^{-1}. Data were fit by the Astra software to the Debye model with a detector fit degree of 2. The *dn/dc* value for the nanoparticles was determined to be 0.14 mL g^{-1}, and the mass concentration used in the calculations was determined from the total amount of CDP-Im and nucleic acid incorporated into the nanoparticles assuming an individual nanoparticle charge ratio of 1.1 (+/-) and complete incorporation of the nucleic acid added during formulation.

4.3.13 Individual nanoparticle stoichiometry

An estimate for the stoichiometry of each nanoparticle (i.e., number of CDP, nucleic acid, AD-PEG, and AD-PEG-Tf molecules) can be calculated from the following equations.

$$MW_{part} = \#NA \times \#bp \times MW_{bp} + \#CDP \times MW_{CDP} + \#PEG \times MW_{PEG} + \#Tf \times MW_{Tf} \quad (4.1)$$

$$CR = \frac{\#CDP}{\#NA \times \#bp} \quad (4.2)$$

$$\#PEG = f_{PEG} \times (100\% - \%Tf) \times \#CDP \times PR \times \frac{FR}{CR} \quad (4.3)$$

$$\#Tf = f_{Tf} \times \%Tf \times \#CDP \times PR \times \frac{FR}{CR} \quad (4.4)$$

where *#NA* is the number of nucleic acid molecules in the nanoparticle, *#CDP* is the number of CDP monomers (β-CD) in the nanoparticle, *#PEG* is the number of AD-PEG molecules in the nanoparticle, *#Tf* is the number of AD-PEG-Tf molecules in the nanoparticle, MW_{part} is the molecular weight of an individual nanoparticle (determined by

MALS), *#bp* is the number of base pairs per nucleic acid molecule (e.g., 21 for siRNA), MW_{bp} is the average molecular weight of each nucleic acid base pair (~650 Da as an approximation), MW_{CDP} is the molecular weight of each CDP monomer (~1,460 Da), MW_{PEG} is the molecular weight of each AD-PEG molecule (~5,200 Da for AD-PEG_{5000}), MW_{Tf} is the molecular weight of each AD-PEG-Tf molecule (~85,000 Da for AD-PEG_{5000}-Tf), f_{PEG} is the fraction of the AD-PEG molecules that bind to nanoparticles during formulation, *PR* is the mole ratio of AD-PEG to β-CD during formulation, *FR* is the formulation charge ratio (+/-), *CR* is the charge ratio (+/- = 1.1) of each individual nanoparticle, f_{Tf} is the fraction of the AD-PEG-Tf molecules that bind to nanoparticles during formulation, and *%Tf* is the mole percent AD-PEG-Tf during formulation.

4.3.14 Salt stability

Particle formulations were diluted to a volume of 1260 μL, placed in a cuvette, and inserted into a ZetaPALS (Brookhaven Instruments Corporation) instrument. Kinetic studies of aggregation were performed by recording the effective diameters at 1 minute intervals after the addition of 1/10 volume 10X PBS to achieve a final concentration of 1X PBS, corresponding to physiological salt concentration.

4.3.15 Erythrocyte aggregation

Erythrocytes were obtained from whole bovine calf blood (Rockland Immunochemicals, Inc.) by multiple rounds of centrifugation at 700x*g* and 4°C for 10 min followed by removal of the supernatant and resuspension of the pellet of erythrocytes in cold PBS (Cellgro) until the supernatant became clear. Finally, the erythrocytes were resuspended at a concentration of 1% (v/v). The free polycations or formulated nanoparticles were added to a 24-well plate and diluted with PBS to a volume of 100 μL.

Subsequently, 100 μL of the erythrocyte suspension were added to each well and the plate was incubated for 1 h at 37°C. Images were taken of each well using a CCD-IRIS/RGB (Sony) video camera attached to an Eclipse TE-300 (Nikon) inverted microscope to visually determine the degree of aggregation.

4.3.16 Complement fixation

To test the complement fixation by polycations or CDP-based nanoparticles, antibody-sensitized sheep erythrocytes were used in a CH50 assay modified from Plank et al. (11). 25 μL human complement sera (Sigma) in gelatin veronal buffer (Sigma) were added in a 1:1.5 dilution series across a row of wells in a 96-well plate. To this same row of wells were added 25 μL of the desired concentration of polycation in its free form or complexed with calf thymus DNA (CT-DNA). A different concentration of the polycations or nanoparticles was added to each row of wells. After a 30-min incubation at 37°C, 1.25×10^7 antibody-sensitized sheep erythrocytes (Sigma) were added to each well and the plate was incubated with shaking for 1 h at 37°C. Finally, the plate was centrifuged at 2,000 RPM for 10 min, 100 μL of the supernatant from each well was transferred to a new 96-well plate, and the absorbance at 410 nm was determined using a SpectraMax 190 (Molecular Devices) microplate reader. This wavelength corresponds to an absorbance peak for the hemoglobin that is released after lysis of the erythrocytes. The CH50 unit is used to define the serum dilution required to achieve 50% lysis of the antibody-sensitized sheep erythrocytes. If the substance being tested binds complement proteins to an appreciable degree, it will sequester these complement proteins and prevent them from binding to and lysing the erythrocytes. As a result, a lower serum dilution (CH50) will be required to achieve 50% erythrocyte lysis under these conditions. The

reported *%CH50max* represents the ratio of the CH50 for the substance being tested to the CH50 determined for the complement sera alone (CH50max).

4.3.17 Cellular uptake

Method 1: Flow cytometry

A FACSCalibur (BD Biosciences) flow cytometer was used to detect the uptake of FL-siRNA (fluorescein attached to the 5' end of the sense strand) delivered with or without the CDP-Im delivery vehicle. HeLa cells were seeded at $2x10^4$ cells per well in 24-well plates 2-3 days prior to transfection and grown in medium supplemented with 10% fetal bovine serum (FBS) and antibiotics (penicillin/streptomycin). The growth medium was removed from each well and replaced with 200 μL Opti-MEM I (Invitrogen), 200 μL Opti-MEM I with 100 nM FL-siRNA, or 200 μL Opti-MEM I with 100 nM FL-siRNA formulated into CDP-Im nanoparticles at a charge ratio of 3 (+/-). After incubation for 2 h at 37°C and 5% CO_2, the transfection medium was removed and the cells were trypsinized and resuspended in Hanks Balanced Salt Solution (HBSS) with 1% bovine serum albumin (BSA) and 10 μg mL^{-1} propidium iodide to detect cell viability.

Method 2: Confocal microscopy

HeLa cells were seeded at $2x10^4$ cells per well in a LabTek II Chamber Slide 2 days prior to transfection and grown in medium supplemented with 10% FBS and antibiotics (penicillin/streptomycin). The growth medium was removed from each well and replaced with 200 μL Opti-MEM I containing 100 nM FL-siRNA formulated into CDP-Im nanoparticles at a charge ratio of 3 (+/-). After incubation for 2 h at 37°C and 5% CO_2, cells were fixed for 15 min at room temperature using 4% paraformaldehyde in

PBS. F-actin was stained with rhodamine phalloidin (Invitrogen) according to manufacturer's instructions. Cells were mounted with Biomeda Gel/Mount according to manufacturer's instructions and the coverslips were subsequently sealed using nail polish. Fluorescent images were acquired using a Zeiss LSM 510 Meta laser scanning confocal microscope with a 40X water-immersion objective.

4.3.18 Competitive uptake

Competitive uptake studies were conducted to determine the impact of free holo-transferrin (holo-Tf) on the relative uptake of transferrin-targeted (containing 1 mol% AD-PEG_{5000}-Tf) or non-targeted nanoparticles. By formulating the nanoparticles with Cy3-siRNA (Cy3 attached to the 5' end of the sense strand), a Tecan SPECTRAFluorPlus plate reader could be used to measure the total cell-associated fluorescence after transfection. Cells were seeded at $2x10^4$ cells per well in 24-well plates 2-3 days prior to transfection and grown in medium supplemented with 10% FBS and antibiotics (penicillin/streptomycin). The growth medium was removed from each well and replaced with 200 μL Opti-MEM I containing 100 nM Cy3-siRNA formulated in nanoparticles. After incubation for 30 min at 37°C and 5% CO_2, the transfection medium was removed and the cells were lysed in 100 μL cell lysate buffer (Promega). Total fluorescence in the 100 μL lysate per well was measured with the SPECTRAFluorPlus plate reader and the number of siRNA molecules was estimated from a standard curve of Cy3-siRNA. Cells in two wells that were not transfected were trypsinized and counted to provide an estimate for the average number of cells per well.

4.3.19 Avidity effects

Method 1: Competitive cell-surface transferrin receptor (TfR) binding assay

Competitive uptake experiments were performed using flow cytometry to detect the uptake of fluorescently labeled holo-Tf. Unlabeled holo-Tf, Tf conjugates (AD-PEG_{5000}-Tf), or Tf-targeted siRNA nanoparticles (1 mol% AD-PEG_{5000}-Tf) were used to compete for uptake by the transferrin receptors on the surface of HeLa cells. Cells were seeded at $2x10^4$ cells per well in 24-well plates 2-3 days prior to transfection and grown in medium supplemented with 10% FBS and antibiotics (penicillin/streptomycin). The growth medium was removed from each well and replaced with 200 μL Opti-MEM I containing 1% BSA, 20 nM AlexaFluor488-labeled holo-Tf (AF488-Tf), and the desired unlabeled Tf competitor. After incubation for 1 h at 37°C and 5% CO_2, the transfection medium was removed and the cells were trypsinized and resuspended in Hanks Balanced Salt Solution (HBSS) with 1% bovine serum albumin (BSA) and 10 μg mL^{-1} propidium iodide to detect cell viability. To enable direct comparison of the effects of avidity, the total amount of Tf was kept constant whether it was in its free form, as AD-PEG_{5000}-Tf, or as AD-PEG_{5000}-Tf on the siRNA nanoparticles. The relative uptake under each condition is reported as the ratio of the mean fluorescence of the wells with unlabeled competitor to the mean fluorescence of the wells with AF488-Tf alone.

Method 2: Live-cell binding assay

A live-cell binding assay was used to measure the relative binding of transferrin-targeted siRNA nanoparticles. $3x10^5$ HeLa cells were resuspended in 100 μL PBS in individual microcentrifuge tubes and cooled on ice. To each microcentrifuge tube were added 100 μL PBS containing PEGylated or Tf-targeted nanoparticles formulated with Cy3-labeled siRNA such that the final Cy3-siRNA concentration was 100 nM. After incubating for 30 minutes on ice, the microcentrifuge tubes were centrifuged for 5

minutes at 200x*g* to pellet the cells. 100 μL of the supernatant from each microcentrifuge tube were added to a well in a black 96-well plate, and the Cy3 fluorescence was measured using a Tecan Safire plate reader. Comparison to a standard curve of Cy3-siRNA nanoparticles allowed quantification of the amount of Cy3-siRNA in each well, and the percent bound (fraction associated with the cell pellet) was determined by subtracting the fluorescence remaining in the supernatant from the initial amount added.

4.3.20 Luciferase knockdown after siRNA transfection

Functional efficacy of pDNA and siRNA delivered by CDP-Im nanoparticles was demonstrated in HeLa cells by co-transfecting the pGL3-CV vector (Promega) containing the firefly luciferase gene and a non-targeting control siRNA (siCON1) synthesized by Dharmacon or a luciferase-targeting siRNA (siLuc) synthesized by Integrated DNA Technologies. The sequence of the siCON1 siRNA is UAGCGACUAAACACAUCAAUU (sense) and UUGAUGUGUUUAGUCGCUAUU (antisense). The sequence of the siLuc siRNA is GUGCCAGAGUCCUUCGAUAdTdT (sense) and UAUCGAAGGACUCUGGCACdTdT (antisense). The Promega Luciferase Assay System was then used to quantify the relative luciferase expression in cells that had been transfected with 1 μg pGL3-CV alone, 1 μg pGL3-CV and 100 nM siCON1, or 1 μg pGL3-CV and 100 nM siLuc. HeLa cells were seeded at $2x10^4$ cells per well in 24-well plates 2-3 days prior to transfection and grown in medium supplemented with 10% FBS and antibiotics (penicillin/streptomycin). CDP-Im nanoparticles were formulated to contain 1 μg pGL3-CV vector and 100 nM siRNA in 200 μL Opti-MEM I. The growth medium was removed from each well and replaced with 200 μL Opti-MEM I containing the formulated nanoparticles. After incubation for 5 h at 37°C and 5% CO_2, 800 μL

complete growth medium was added to each well. 48 h later, the cells were lysed in 100 μL 1X Luciferase Cell Culture Lysis Reagent (Promega). 10 μL of the cell lysate were added to 90 μL of the luciferase substrate, and bioluminescence was measured using a MonoLight (Pharmingen) luminometer. 5 μL of the cell lysate were used in a BioRad DC protein assay to determine the protein concentration in each lysate sample. Luciferase activities are reported as relative light units per mg protein.

4.4 Results and discussion

4.4.1 Particle formation requires a slight excess of positive charge and protects siRNA from degradation in serum

Results from an electrophoretic mobility shift assay (EMSA) demonstrate that siRNA nanoparticles completely form at charge ratios (+/-) greater than ~1 to 1.5 (Figure 4.2A). At sufficiently high charge ratios, the band corresponding to the free nucleic acid becomes undetectable since the nucleic acid remains associated with the nanoparticles that have greatly reduced electrophoretic mobility. To determine what portion of the polycations (CDP) added during formulation actually are incorporated into the nanoparticles, the free polycations were separated from the nanoparticles after formulation. Regardless of the formulation charge ratio up to 30 (+/-), the charge ratio of individual nanoparticles remains ~1 (+/-) (Figure 4.2B). This is consistent with the results shown in Figure 4.2A where charge ratios slightly greater than 1 were required to achieve complete nanoparticle formation. A nuclease stability assay was conducted to determine if the formation of nanoparticles could protect the nucleic acid payload from degradation by nucleases present in serum. While naked siRNA degrades rapidly in serum, siRNA within nanoparticles is protected from significant degradation even after 4

hours in 50% mouse serum (Figure 4.3). Additionally, the data given in Figure 4.3 show (i) there is essentially complete encapsulation of the siRNA by the nanoparticles, and (ii) when the nanoparticles exposed to serum are disrupted with SDS, the nucleic acids released are still intact siRNA duplexes.

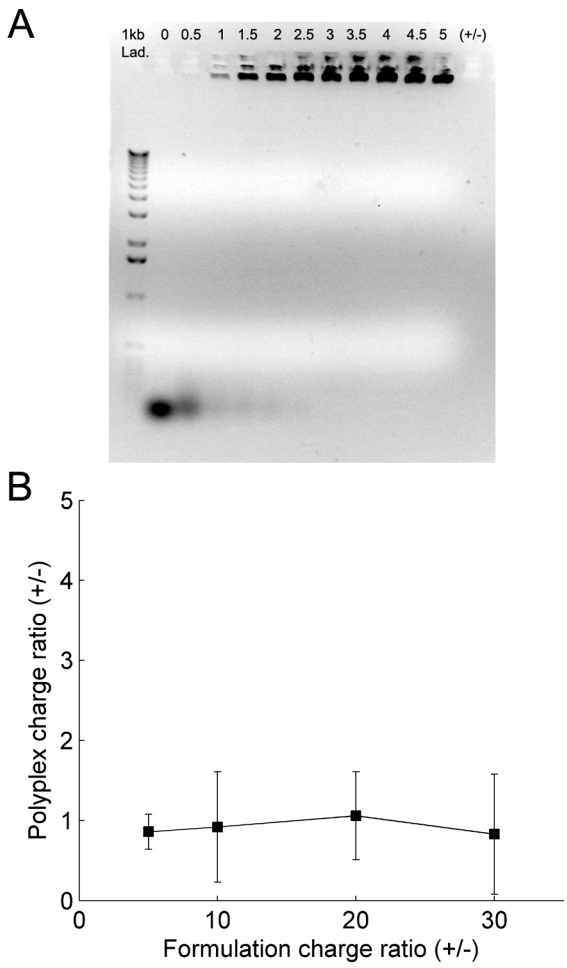

Figure 4.2. Effect of formulation charge ratio (+/-). (A) Electrophoretic gel mobility shift assay demonstrating the effect of formulation charge ratio on siRNA nanoparticle formation. (B) Individual nanoparticle charge ratio as a function of formulation charge ratio.

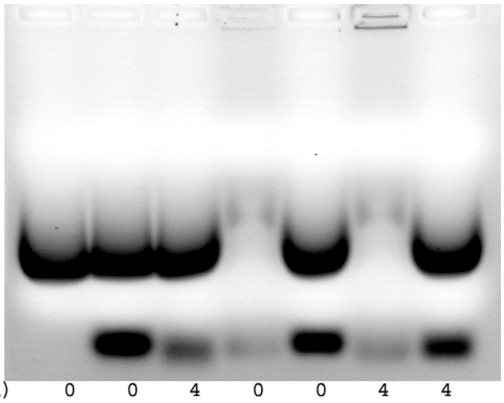

Time(h)	0	0	4	0	0	4	4
CDPIm	-	-	-	+	+	+	+
siRNA	-	+	+	+	+	+	+
SDS	+	+	+	-	+	-	+
Serum	+	+	+	+	+	+	+

Figure 4.3. Nuclease stability of siRNA encapsulated within nanoparticles. For the t = 4 lanes, naked siRNA or siRNA within CDP-Im nanoparticles (3 (+/-)) was incubated in 50% mouse serum for 4 h at 37°C and 5% CO_2. For the t = 0 lanes, serum was added to an equivalent amount of naked siRNA or siRNA within CDP-Im nanoparticles immediately before loading into the gel. Addition of 1% SDS was used to displace the siRNA from the nanoparticles to visualize the amount of intact siRNA remaining. The first lane demonstrates that the upper bands are nonspecific bands resulting from the interaction between SDS, serum, and the ethidium bromide stain, while the lower bands correspond to the free siRNA.

4.4.2 Formulation conditions affect nanoparticle size and zeta potential

Transmission electron microscopy (TEM) and atomic force microscopy (AFM) were used to visualize the siRNA nanoparticles formulated at a charge ratio of 3 (+/-). The images in Figure 4.4 demonstrate that the siRNA nanoparticles assume a roughly spherical shape, but the unPEGylated nanoparticles display more variability in size and adopt a slightly oblong shape relative to the PEGylated nanoparticles when they are visualized by AFM on the mica surface. While a large fraction of the unPEGylated nanoparticles (0.1 g L^{-1} siRNA) have diameters that exceed 100 nm, PEGylated nanoparticles (0.5 g L^{-1} siRNA) formulated with a 1:1 mole ratio of AD-PEG_{5000}:β-CD consistently have diameters <100 nm and are approximately 60-80 nm.

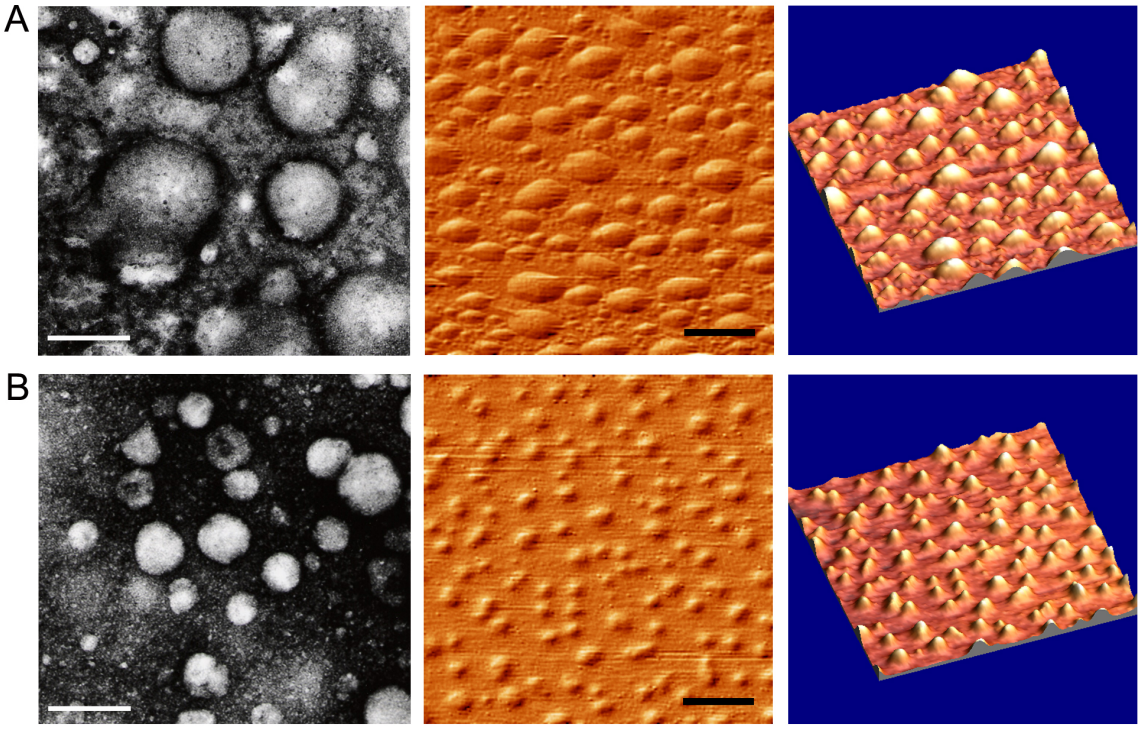

Figure 4.4. Transmission electron microscopy (left panels) and atomic force microscopy (center and right panels) images of (A) unPEGylated and (B) PEGylated siRNA nanoparticles formulated at a charge ratio of 3 (+/-). Scale bar = 100 nm (left panels) and 200 nm (center and right panels).

To further investigate the effects of formulation conditions, dynamic light scattering was used to measure the effective hydrodynamic diameter and zeta potential of the nanoparticles. Consistent with the TEM and AFM images, the results shown in Figure 4.5A reveal that the nucleic acid concentration during formulation affects the size of the nanoparticles. Nanoparticles formulated with siRNA, pDNA, and calf thymus (CT-DNA) show nearly identical trends of increased size with higher nucleic acid concentration. However, nanoparticles that are formulated in the presence of AD-PEG_{5000} (PEGylated nanoparticles formed by the pre-complexation method) do not exhibit such a dependence on formulation conditions (Figure 4.5B).

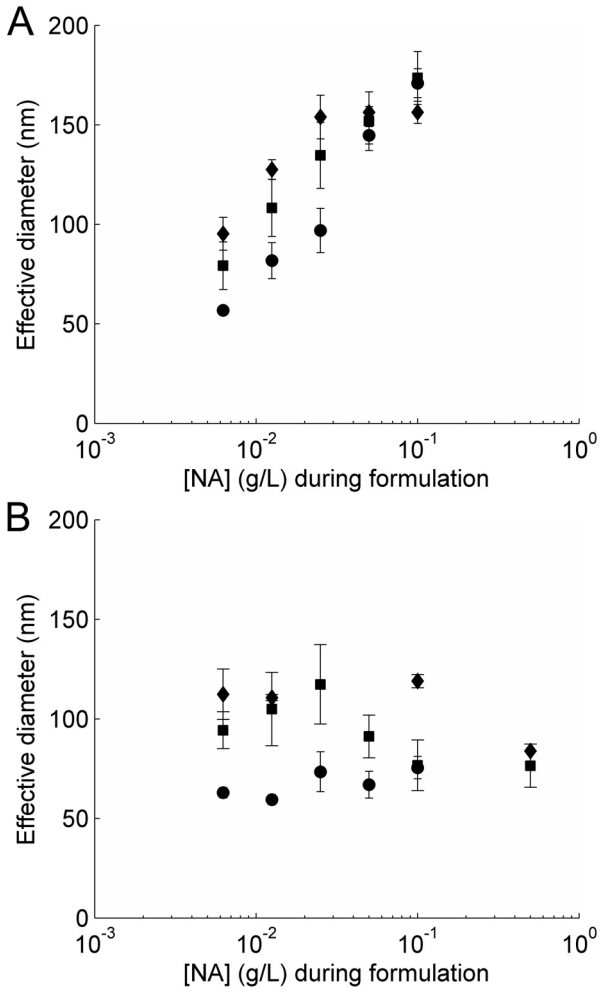

Figure 4.5. Effect of nucleic acid concentration ([NA]) during formulation on the size of (A) unPEGylated or (B) PEGylated nanoparticles. Nanoparticles were formulated at a charge ratio of 3 (+/-) using CDP-Im and either siRNA, pDNA, or CT-DNA (calf thymus DNA). PEGylated nanoparticles were formulated by adding a 1:1 mole ratio of AD-PEG_{5000}:β-CD. Nanoparticle effective diameter was determined using dynamic light scattering. Squares = CDP-Im/siRNA nanoparticles, circles = CDP-Im/pDNA nanoparticles, diamonds = CDP-Im/CT-DNA nanoparticles.

These properties allow the delivery vehicles to be fine-tuned with respect to size by altering the formulation conditions accordingly (i.e., PEGylation through the pre- or post-complexation method). The zeta potential of unPEGylated nanoparticles ranges from 10 (particles ~60 nm in diameter) to 30 mV (particles ~150 nm in diameter), while that of PEGylated nanoparticles ranges from 10 to 20 mV for similarly sized nanoparticles. This positive zeta potential implies that the charge ratio of the individual

nanoparticles is slightly greater than 1 (+/-). The AD-PEG$_{5000}$ conjugates can be further modified to contain targeting ligands on the distal end of the PEG chain. For example, transferrin can be conjugated to the AD-PEG$_{5000}$ molecules to yield AD-PEG$_{5000}$-Tf (19). Because the transferrin protein is negatively charged, inclusion of AD-PEG$_{5000}$-Tf molecules during nanoparticle formulation reduces the zeta potential of siRNA nanoparticles in a concentration-dependent manner (Figure 4.6). Bellocq et al. reported a similar trend using nanoparticles made with pDNA (19).

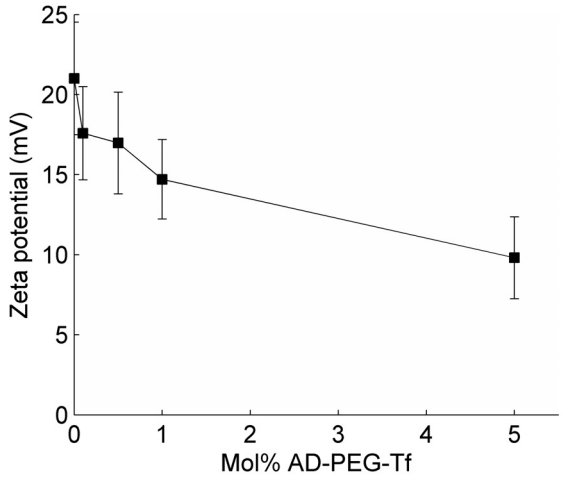

Figure 4.6. Nanoparticle zeta potential as a function of AD-PEG$_{5000}$-Tf ligand concentration during formulation. Nanoparticles were formulated at a charge ratio of 3 (+/-) using CDP-Im and siRNA, and the AD-PEG$_{5000}$ or AD-PEG$_{5000}$-Tf molecules were added after nanoparticle formation (post-complexation). The total number of moles of AD-PEG$_{5000}$-X (AD-PEG$_{5000}$ and AD-PEG$_{5000}$-Tf) was equal to the number of moles of β-CD, and the mixture of AD-PEG$_{5000}$ and AD-PEG$_{5000}$-Tf is defined by the % AD-PEG$_{5000}$-Tf.

4.4.3 AD-PEG conjugates bind to the surface of nanoparticles through inclusion complex formation

An important property of the cyclodextrin-containing polycations is their ability to form inclusion complexes with hydrophobic molecules. This provides the opportunity for modular attachment of different stabilizing molecules or targeting ligands through coupling to an adamantane (AD) molecule that forms inclusion complexes with the β-

cyclodextrin molecules. Isothermal titration calorimetry was used to investigate the thermodynamics of the interaction between AD-PEG molecules and CDP-Im either in its free form or within siRNA-containing nanoparticles (Table 4.1).

Table 4.1. Measured ITC parameters for the binding between AD-PEG_{5000} and β-CD alone, polycation alone (CDP-Im), or CDP-Im/siRNA nanoparticles formulated at charge ratios from 3 to 15 (+/-). For comparison, literature values are provided for the binding between β-CD alone and adamantane carboxylate (22).

β-CD + adamantane carboxylate			
	n	***K* (M^{-1})**	***ΔH* (cal M^{-1})**
β-CD	1	42000	-4440
β-CD + AD-PEG_{5000}			
	n	***K* (M^{-1})**	***ΔH* (cal M^{-1})**
β-CD	1.1	30600	-7358
siRNA nanoparticle + AD-PEG_{5000}			
	n	***K* (M^{-1})**	***ΔH* (cal M^{-1})**
3 (+/-)	0.34 ± 0.09	5110 ± 730	-15200 ± 4090
5 (+/-)	0.38 ± 0.04	6320 ± 330	-12600 ± 570
10 (+/-)	0.48 ± 0.02	8090 ± 620	-10100 ± 520
15 (+/-)	0.49 ± 0.01	8050 ± 800	-10600 ± 450
CDP-Im	0.54 ± 0.04	8380 ± 940	-9460 ± 1490

Figure 4.7 shows representative ITC data plots for binding between AD-PEG_{5000} and CDP-Im formulated with siRNA at a charge ratio of 3 (+/-), CDP-Im formulated with siRNA at a charge ratio of 10 (+/-), and CDP-Im alone. As the charge ratio increases, the measured binding parameters approach those of free CDP-Im. Given the previous results showing the actual nanoparticle charge ratio is slightly greater than 1 (+/-), this is consistent with the presence of excess free CDP-Im at charge ratios >1.

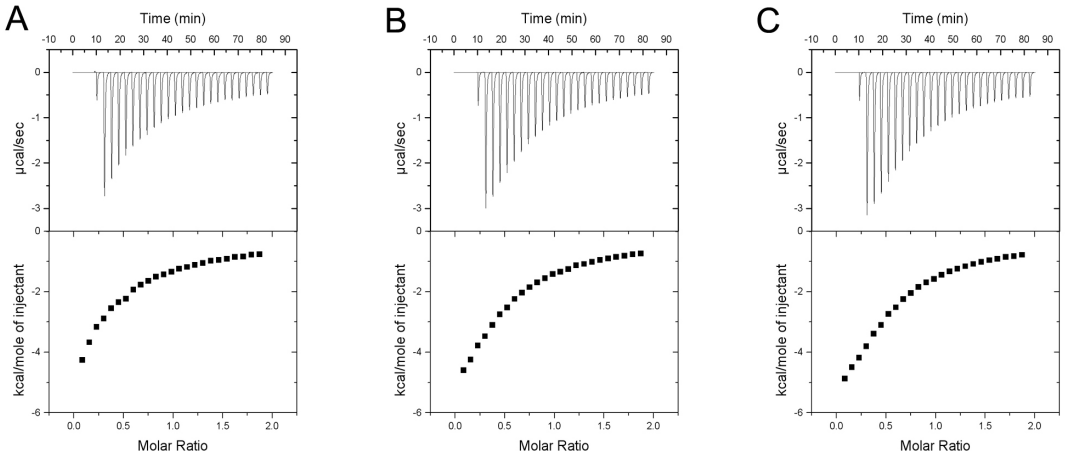

Figure 4.7. Isothermal titration calorimetry (ITC) plots characterizing the binding between AD-PEG_{5000} molecules and free CDP-Im or siRNA nanoparticles. (A) CDP-Im/siRNA nanoparticle (3 (+/-)) and AD-PEG_{5000}, (B) CDP-Im/siRNA nanoparticle (10 (+/-)) and AD-PEG_{5000}, (C) CDP-Im and AD-PEG_{5000}.

The value of *n* represents the fraction of the β-CD molecules available for inclusion complex formation with the AD-PEG molecules. Each β-CD cup can interact with a single adamantane molecule, as previous reports have shown a 1:1 binding stoichiometry between adamantane molecules and β-CD (*22*). While binding between individual β-cyclodextrins and AD-PEG_{5000} conjugates gives the expected *n* value of ~1, binding between CDP-Im and AD-PEG_{5000} exhibits an *n* value of ~0.5. When the AD-PEG_{5000} molecule containing a 5000-Da PEG chain binds to a β-CD cup on the CDP-Im polymer, it likely provides steric hindrance that impedes binding between other AD-PEG_{5000} molecules and nearby β-CD molecules. Support for this hypothesis comes from the observation that the *n* value for binding between CDP-Im and AD-PEG_{500} molecules containing short 500-Da PEG chains is 0.92 ± 0.05, likely indicating that the shorter PEG chains do not interfere to as great an extent with the binding of AD-PEG_{500} to neighboring β-CD molecules.

Another interesting pattern is observed with the ΔH values, representing the change in enthalpy that results from binding between an AD-PEG molecule and a β-CD cup. These values are all negative, indicating that energy is released upon binding due to the favorable interaction between the hydrophobic adamantane and the β-CD cup. Notably, ΔH is more negative for AD-PEG_{5000} binding to the siRNA nanoparticles than it is for AD-PEG_{5000} binding to free CDP-Im. We hypothesize that this increased stabilization energy, in addition to the inclusion complex formation, is a result of favorable interactions between the PEG chains themselves when they are grouped together on the surface of an siRNA nanoparticle.

4.4.4 Particle molecular weight can be used to estimate individual nanoparticle stoichiometry

Determining the individual component stoichiometry of the nanoparticles provides important insights into their functional properties. Centrifugal filtration was used to separate unbound components from those bound to the nanoparticles. As discussed previously, it was determined that the individual nanoparticle charge ratio (i.e., the ratio of positive charges from the CDP-Im to negative charges from the nucleic acid) is slightly greater than 1; we used 1.1 (+/-) for the calculations. The percent of the total AD-PEG_{5000} or AD-PEG_{5000}-Tf added to the formulation mixture that remains free was determined by quantifying the AD-PEG_{5000} (experiment actually used AD-PEG_{5000}-Lac and we assumed that the value for AD-PEG_{5000} would be approximately the same) or AD-PEG_{5000}-Tf recovered in the filtrate versus the retentate after centrifugal filtration. The results of these measurements indicated that approximately 3% of the total AD-PEG_{5000} and 10% of the total AD-PEG_{5000}-Tf added during formulation remained associated with

the nanoparticles. The greater degree of binding measured for the AD-PEG_{5000}-Tf conjugates may be partly due to charge interactions between the negatively charged transferrin proteins and the positively charged nanoparticles. The final piece of data needed to estimate the individual nanoparticle stoichiometry is the molecular weight of the nanoparticles. This was determined using multi-angle light scattering. The results in Figure 4.8 show that the molecular weight of nanoparticles formulated with siRNA, pDNA, or calf thymus (CT-DNA) scales approximately as r^3, where r is the radius of the nanoparticle determined by DLS.

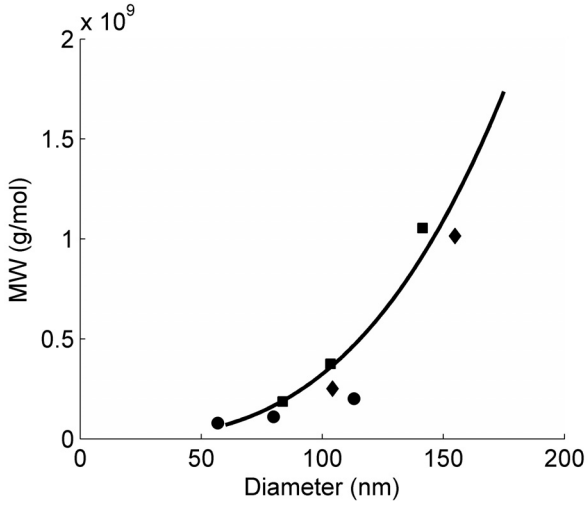

Figure 4.8. Relationship between nanoparticle size and molecular weight (MW) as determined by dynamic and multi-angle light scattering. Nanoparticles were formulated at a charge ratio of 3 (+/-) using CDP-Im and either siRNA, pDNA, or CT-DNA. Effective diameters were measured using dynamic light scattering, and molecular weights were determined using multi-angle light scattering. Squares = CDP-Im/siRNA nanoparticles, circles = CDP-Im/pDNA nanoparticles, diamonds = CDP-Im/CT-DNA nanoparticles, solid line = r^3 scaling dependence of the MW of nanoparticles starting with a MW of $7x10^7$ g mol^{-1} for a 60-nm nanoparticle.

This similarity between all three types of nanoparticles is consistent with the trends observed in Figure 4.5, further supporting the interesting result that formulation with a variety of nucleic acids leads to nanoparticles with similar physical properties. An unPEGylated nanoparticle with a diameter of 70 nm is expected to have a molecular

weight around $1x10^8$ g mol^{-1} from data given in Figure 4.8. Inserting this molecular weight and an individual nanoparticle charge ratio of 1.1 (+/-) into Equations 1 and 2 yields 48,800 CDP monomers (or 9,750 CDP chains with a degree of polymerization of 5) and 2,110 siRNA molecules (with 21 bp per siRNA) per nanoparticle. For the sake of calculation, we can then use this value for *#CDP* to estimate the number of AD-PEG_{5000} and AD-PEG_{5000}-Tf molecules per nanoparticle using Equations 3 and 4. For example, a 70-nm siRNA nanoparticle with a molecular weight of $1.3x10^8$ g mol^{-1} (accounting for the added mass from the PEG conjugates) formulated at a charge ratio of 3 (+/-) with 1 mol% AD-PEG_{5000}-Tf is calculated to contain 9,750 CDP chains, 2,110 siRNA molecules, 3,950 AD-PEG_{5000} molecules, and 133 AD-PEG_{5000}-Tf molecules.

By approximating each siRNA molecule as a cylinder with a diameter of 2.37 nm and a length of 7.14 nm (approximated based on the dimensions of a double-stranded DNA helix), each siRNA molecule can be estimated to occupy a volume of $3.15x10^{-25}$ m^3. Therefore, 2,110 siRNA molecules would occupy a minimum volume of $6.7x10^{-23}$ m^3; this represents approximately 37% of the total nanoparticle volume of $1.8x10^{-22}$ m^3 for a 70-nm sphere. Therefore, this number of siRNA molecules appears to be reasonable given the size constraints of the nanoparticles. Furthermore, the corresponding surface density for the estimated number of AD-PEG_{5000} chains on a 70-nm nanoparticle is ~43 pmol cm^{-2} or 0.26 chains nm^{-2}. The calculated average distance between PEG_{5000} molecules at this surface density is ~2.0 nm, while the Flory radius is ~6 nm. Since the distance between PEG_{5000} molecules is much less than the Flory radius, the PEG_{5000} chains are expected to interact laterally and extend out from the surface in a dense brush layer with an estimated thickness of ~12.5 nm. Hansen et al. further examined the brush

scaling laws for polyethylene glycols and predicted that PEG_{5000} solutions must have monomer volume fractions, ϕ, greater than 0.07-0.09 to be in the brush regime (23). This is satisfied when the PEG_{5000} surface density exceeds ~26-28 pmol cm^{-2}, again indicating that the PEG_{5000} chains on the nanoparticles are in the brush regime.

4.4.5 PEGylation provides steric stabilization to the nanoparticles and reduces nonspecific interactions

DLS-based kinetic studies of aggregation were performed to determine whether the inclusion of AD-PEG conjugates could help to stabilize the nanoparticles against aggregation at physiological salt concentrations. First, the ratio of AD-PEG_{5000}:β-CD (mol:mol) was varied from 0 to 2 to investigate how the surface density of AD-PEG_{5000} affects the steric stability of siRNA nanoparticles formulated through the post-complexation method (Figure 4.9A). Nanoparticles formulated with AD-PEG_{5000}:β-CD (mol:mol) ratios >1 do not exhibit observable aggregation after 15 minutes in 1X PBS. At ratios <1, aggregation increases as the ratio of AD-PEG_{5000}:β-CD (mol:mol) decreases. These results with siRNA-containing nanoparticles are consistent with those observed by Pun et al. using nanoparticles made with pDNA (24). The length of the PEG molecule in the AD-PEG conjugate also impacts its ability to confer steric stabilization to the nanoparticles. As shown in Figure 4.9B, the stabilization effects increase with the length of the PEG chain, with AD-PEG_{500} (AD-PEG_{500}:β-CD = 1) only slightly slowing the aggregation while AD-PEG_{5000} (AD-PEG_{5000}:β-CD = 1) prevents detectable aggregation up to 15 minutes after salt addition. If the AD-PEG_{500} chains, like the AD-PEG_{5000} chains, also achieve a surface density of ~43 pmol cm^{-2} (AD-PEG_{500}:β-CD = 1), then the average distance between PEG_{500} chains remains ~2.0 nm. However, since this

is not less than the Flory radius for a PEG_{500} molecule (~1.5 nm), the PEG_{500} molecules are not expected to form the brush-like layer on the nanoparticle surface that is needed for steric stabilization. Furthermore, modification of up to 1 mol% of the AD-PEG_{5000} chains with Tf (AD-PEG_{5000}-Tf) leads to minimal perturbations in the salt stability of the nanoparticles. However, at 5 mol% AD-PEG_{5000}-Tf, gradual nanoparticle aggregation becomes apparent during the 15-minute incubation in 1X PBS.

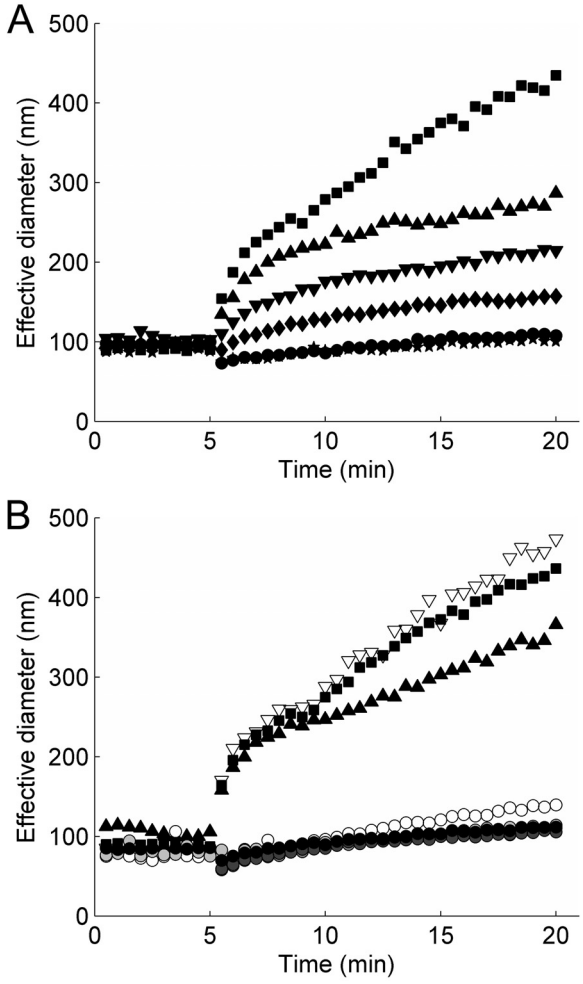

Figure 4.9. Aggregation of siRNA nanoparticles in physiological salt solutions. 140 μL of a 10X PBS solution were added to 1260 μL of the nanoparticles in water after 5 minutes, and dynamic light scattering was used to follow the formation of aggregates with time. (A) Effect of the ratio of AD-PEG_{5000}:β-CD on nanoparticle stability. CDP-Im/siRNA (3 (+/-)) nanoparticles were formulated without AD-PEG_{5000} (black squares) or through the post-complexation method with an AD-PEG_{5000}:β-CD mole ratio of 0.25:1 (black triangles), 0.5:1 (inverted black triangles), 0.75:1 (black diamonds), 1:1 (black circles), or 2:1 (black stars). (B) Effect of PEG chain length, adamantane conjugation, and Tf targeting ligand density on nanoparticle

stability. CDP-Im/siRNA (3 (+/-)) nanoparticles were formulated without AD-PEG_{5000} (black squares), with a PEG_{5000} (no adamantane):β-CD mole ratio of 1:1 (open inverted triangles), with an AD-PEG_{500}:β-CD mole ratio of 1:1 (black triangles), with an AD-PEG_{5000}:β-CD mole ratio of 1:1 (black circles), or with a 1:1 mole ratio of AD-PEG_{5000}-X:β-CD where AD-PEG_{5000}-X was composed of 0.1 wt% AD-PEG_{5000}-Tf (dark gray circles), 0.1 mol% AD-PEG_{5000}-Tf (gray circles), 1 mol% AD-PEG_{5000}-Tf (light gray circles), or 5 mol% AD-PEG_{5000}-Tf (open circles) and the remainder AD-PEG_{5000}.

Besides providing steric stabilization to the nanoparticles, PEGylation can help to reduce nonspecific interactions. Specifically, experiments were performed to study the interaction between the polycations (or nanoparticles) and erythrocytes (Figure 4.10). Significant erythrocyte binding will lead to aggregation that can be observed by visual inspection using a light microscope. While the free CDP or CDP-Im showed negligible aggregation at 0.2 g L^{-1}, some aggregation was observed as the concentration increased to 2 g L^{-1} (Figure 4.10A-D). Erythrocyte aggregation was also measured after incubation with siRNA nanoparticles that were formulated with CDP-Im and a 1:1 mole ratio of AD-PEG_{5000}:CDP-Im (Figure 4.10E). The results demonstrate that PEGylated nanoparticles do not lead to any observable aggregation at a total CDP-Im concentration of 0.2 g L^{-1}, corresponding to the expected concentration after systemic delivery in vivo (7).

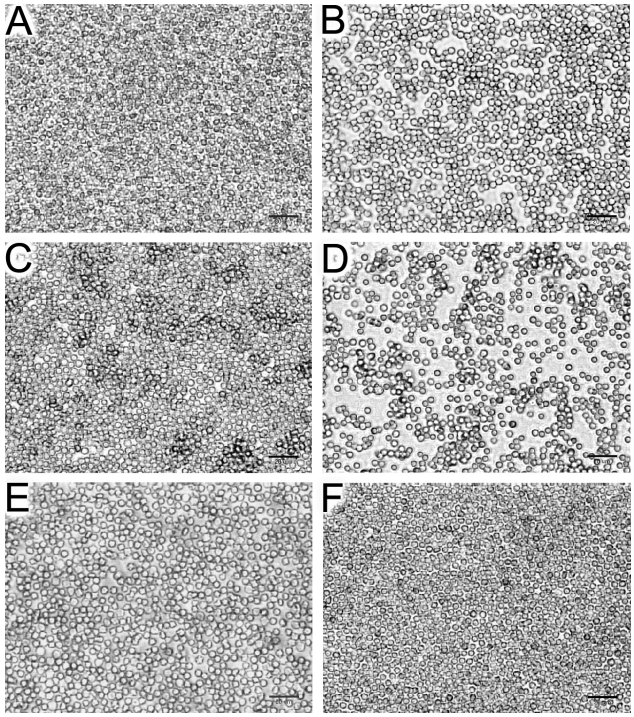

Figure 4.10. Erythrocyte aggregation. (A) 0.2 g L^{-1} CDP, (B) 2 g L^{-1} CDP, (C) 0.2 g L^{-1} CDP-Im, (D) 2 g L^{-1} CDP-Im, (E) CDP-Im/siRNA (3 (+/-)) nanoparticles at 0.2 g L^{-1} CDP-Im formulated with a 1:1 mole ratio of AD-PEG_{5000}:β-CD, (F) PBS alone. Scale bar = 20 μm.

4.4.6 PEGylated nanoparticles show minimal complement fixation

Complement fixation by polyethylenimine and polylysine was compared to that of CDP or CDP-Im. The CDP and CDP-Im molecules do not show as much complement fixation as PEI (branched or linear) or a 36-mer of polylysine, but they do exhibit higher complement fixation than a 5-mer of polylysine (Figure 4.11A). This is consistent with the notion that polycation length and charge density can augment complement activation (11).

Because complement fixation was observed at the physiologically relevant concentration of 0.2 g L^{-1}, corresponding to the typical concentration of polycations in the bloodstream after delivery of nucleic acids at a dose of 2.5 mg kg^{-1} (a typical dose used for in vivo siRNA delivery (7)), experiments were performed to test nanoparticles

formulated with calf thymus DNA and stabilized by PEGylation (Figure 4.11B). Notably, these formulations showed minimal complement fixation at polymer concentrations of 0.2 g L^{-1}.

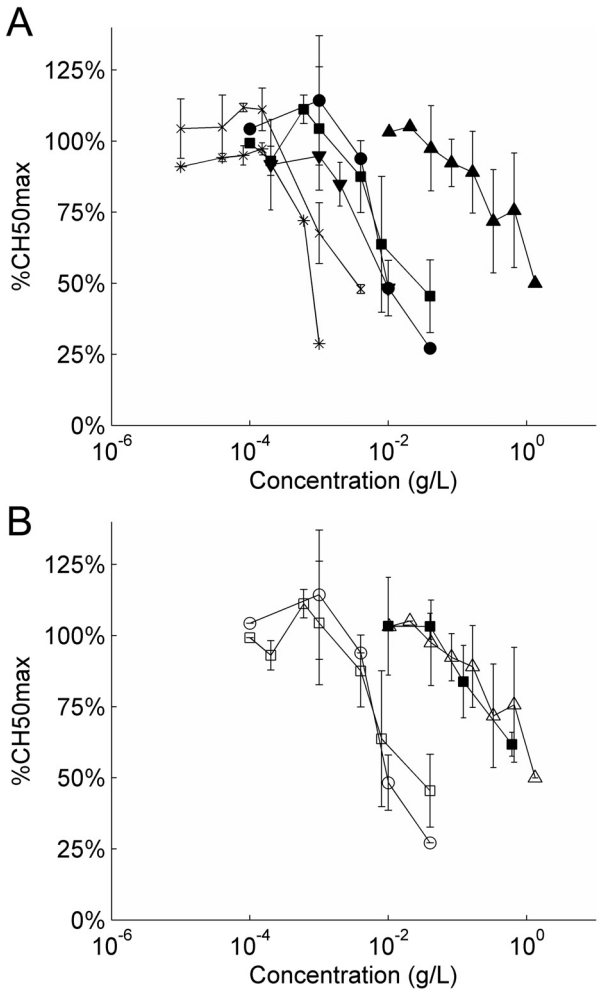

Figure 4.11. Complement fixation. (A) Complement fixation by free polycations. Asterisks = branched PEI, x = linear PEI, black triangles = pentalysine, inverted black triangles = polylysine (36-mer), black squares = CDP, black circles = CDP-Im. (B) Complement fixation by CDP/CT-DNA (3 (+/-)) nanoparticles formulated with a 1:1 mole ratio of AD-PEG_{5000}:β-CD (black squares). The curves for CDP (open squares), CDP-Im (open circles), and pentalysine (open triangles) are shown again for comparison.

4.4.7 Particles achieve intracellular delivery of siRNA in vitro

The uptake of nanoparticles containing fluorescently labeled siRNA was assessed using flow cytometry and confocal fluorescence microscopy. While naked siRNAs do

not achieve measurable levels of cellular uptake, formulation into nanoparticles with CDP-Im dramatically increases the amount of cell-associated siRNA as measured by flow cytometry (Figure 4.12A). To confirm that the siRNA was being delivered to the interior of cells, confocal fluorescence microscopy was used to visualize cells transfected with nanoparticles containing fluorescently labeled siRNA (Figure 4.12B). The internalized nanoparticles exhibited a punctate staining and were eventually observed to accumulate in the perinuclear region.

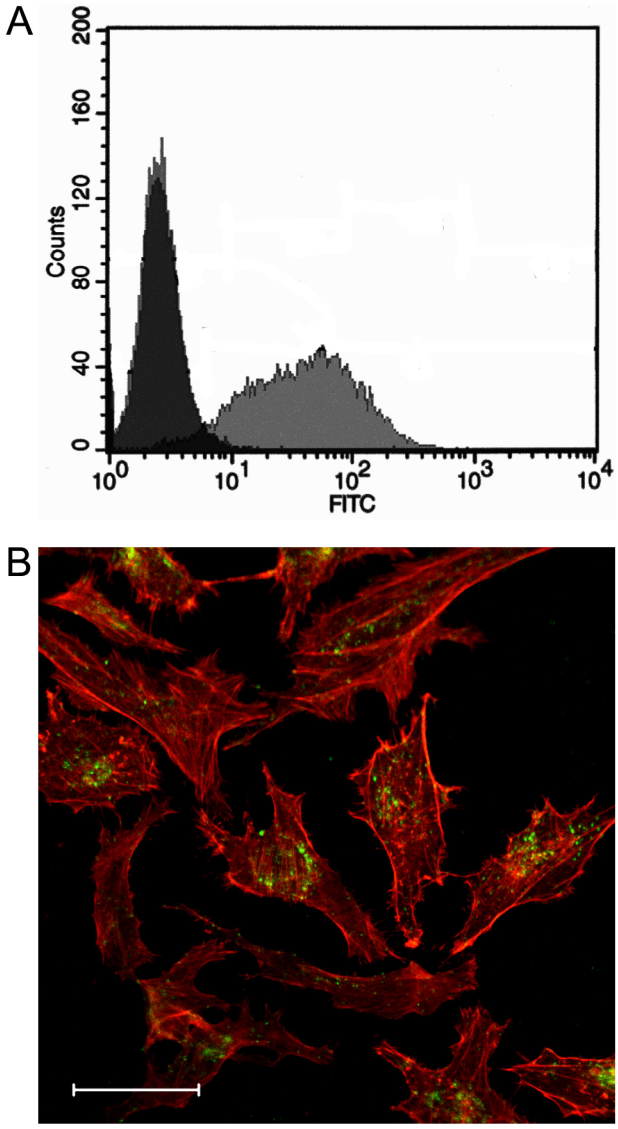

Figure 4.12. Uptake of CDP-Im nanoparticles containing fluorescein (FL)-labeled siRNA by HeLa cells. (A) Histogram of cell-associated fluorescence measured by flow cytometry. The left-most peaks correspond to the overlapping peaks for HeLa cells incubated with either Opti-MEM I alone or 100 nM naked FL-siRNA, while the right-most peak represents the cell-associated fluorescence after transfection with CDP-Im/FL-siRNA nanoparticles. (B) Confocal fluorescence microscopy image of HeLa cells after transfection with CDP-Im/FL-siRNA nanoparticles (green) and rhodamine phalloidin staining of F-actin (red). Scale bar = 50 μm.

4.4.8 Targeting ligands enhance cellular uptake of PEGylated nanoparticles

To verify that attachment of AD-PEG$_{5000}$-Tf can lead to uptake through transferrin receptor (TfR)-mediated endocytosis, the uptake of stabilized (PEGylated)

nanoparticles was measured in the presence or absence of free holo-Tf. While the uptake of PEGylated nanoparticles without AD-PEG_{5000}-Tf was not affected by the presence of free holo-Tf, the uptake of Tf-targeted nanoparticles was reduced as a result of competition with free holo-Tf (Figure 4.13). Because the nanoparticles can be internalized simultaneously by numerous mechanisms including simple pinocytosis, there is still significant uptake even without TfR-mediated internalization under these conditions.

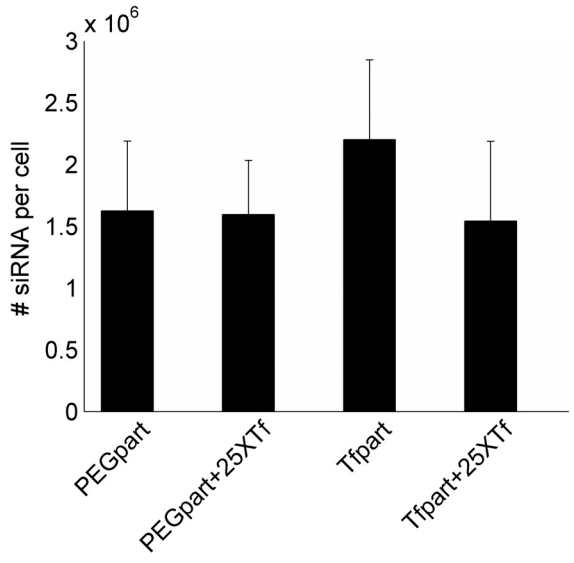

Figure 4.13. Uptake of PEGylated and Tf-targeted nanoparticles in the presence of holo-Tf competitor. Nanoparticles were formulated at a charge ratio of 3 (+/-) using CDP-Im and siRNA. PEGylated nanoparticles (PEGpart) were formulated with a 1:1 mole ratio of AD-PEG_{5000}:β-CD and Tf-targeted nanoparticles (Tfpart) were formulated with a 1:1 mole ratio of AD-PEG_{5000}-X:β-CD where AD-PEG_{5000}-X was composed of 99 mol% AD-PEG_{5000} and 1 mol% AD-PEG_{5000}-Tf. Nanoparticles containing 100 nM siRNA were added to HeLa cells in 200 μL Opti-MEM I in the absence or presence of a 25X (moles holo-Tf: moles AD-PEG_{5000}-Tf) excess of holo-Tf competitor.

4.4.9 Targeted nanoparticles exhibit avidity effects

If multiple receptor/ligand interactions can occur simultaneously, then the effective affinity of the binding interaction can be enhanced through avidity effects. Antibodies or divalent antibody fragments are excellent examples of molecules whose

binding affinities are enhanced through avidity effects. Their divalent interactions allow single antibodies to bind two separate receptors, leading to a stronger apparent affinity than exhibited by the monovalent antibody fragment (25). Targeted delivery vehicles that contain multiple targeting ligands on the surface should also display these avidity effects if multiple targeting ligands can simultaneously interact with the receptors. A typical cancer cell may contain thousands of receptors on its surface (26,27), and the Tf-targeted delivery vehicles can contain tens or even hundreds of Tf ligands (depending on the percent of the AD-PEG_{5000} molecules with Tf molecules attached to the distal end of the flexible PEG_{5000} chains) decorating each nanoparticle surface. This arrangement should enable multiple Tf molecules to bind to TfR on the surface of the cells. To test whether these avidity effects increase the apparent affinity of the Tf-targeted nanoparticles for the TfR on the cell surface, a competitive uptake assay was performed using flow cytometry. The results shown in Figure 4.14A demonstrate that the Tf-targeted nanoparticles possess enhanced affinity for the TfR relative to individual AD-PEG_{5000}-Tf molecules. Additionally, nanoparticles without the Tf targeting ligand had a minimal impact on the uptake of the fluorescently labeled holo-Tf. To determine how targeting ligand density affects nanoparticle binding to cell-surface TfR, nanoparticles were incubated with HeLa cells in PBS at 4°C to measure the amount of binding in the absence of internalization. The results shown in Figure 4.14B show that Tf targeting increases the amount of cell-associated nanoparticles under these conditions, and the amount of binding increases with the targeting ligand density.

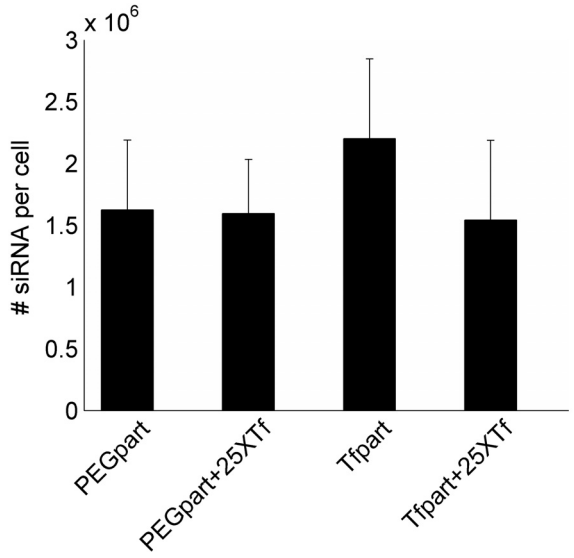

Figure 4.14. Effect of transferrin targeting ligand density on relative binding affinity. (A) Competitive TfR binding by free holo-Tf (circles), free AD-PEG_{5000}-Tf (triangles), Tf-targeted CDP-Im/siRNA (3 (+/-), 1 mol% AD-PEG_{5000}-Tf) nanoparticles (squares), and PEGylated CDP-Im/siRNA (3 (+/-)) nanoparticles (diamonds) in the presence of 20 nM AlexaFluor488-labeled holo-Tf. As a control, the PEGylated nanoparticles were formulated identically to the Tf-targeted nanoparticles at each concentration except without the addition of AD-PEG_{5000}-Tf during formulation. (B) Live-cell binding assay. Nanoparticles were formulated at a charge ratio of 3 (+/-) using CDP-Im and Cy3-labeled siRNA. PEGylated nanoparticles (PEGpart) were formulated with a 1:1 mole ratio of AD-PEG_{5000}:β-CD and Tf-targeted nanoparticles (Tfpart) were formulated with a 1:1 mole ratio of AD-PEG_{5000}-X:β-CD where AD-PEG_{5000}-X was composed of the stated % AD-PEG_{5000}-Tf and the remainder AD-PEG_{5000}. Nanoparticles containing 100 nM Cy3-siRNA were added to HeLa cells in 200 μL PBS and incubated on ice for 30 minutes. The "percent bound" represents the fraction of nanoparticles associated with the cell pellet after centrifugation.

4.4.10 Particles deliver functional pDNA and siRNA to cells in vitro

In addition to achieving intracellular delivery of the nucleic acid-containing nanoparticles, the nanoparticles need to release their nucleic acid payload intracellularly to allow it to function. Co-delivery of a luciferase-expressing plasmid and either a control or luciferase-targeting siRNA was used to demonstrate the ability of the nanoparticles to deliver functional pDNA and siRNA. The luciferase activity in cell lysates was quantified using a luminometer, and relative light units (RLU) were normalized to total cellular protein levels. As shown in Figure 4.15, cells that received

CDP-Im nanoparticles containing the plasmid and siRNA against luciferase (siLuc) had luciferase activity that was ~50% lower than cells that received CDP-Im nanoparticles with either the plasmid alone or the plasmid plus a control siRNA (siCON1).

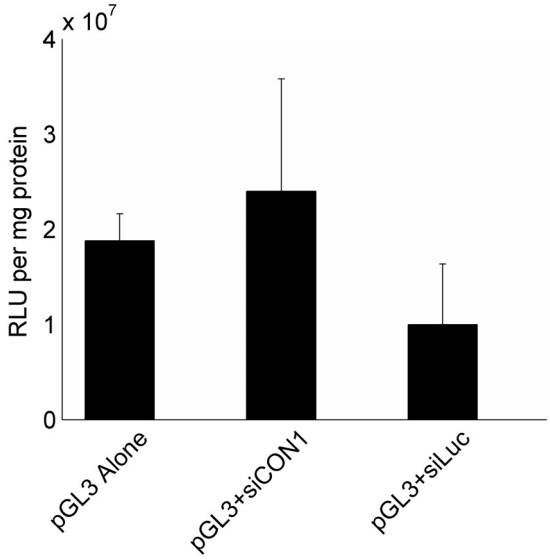

Figure 4.15. Luciferase expression 48 h after co-transfection of HeLa cells with nanoparticles containing pDNA and siRNA. Nanoparticles were formulated at a charge ratio of 3 (+/-) by combining CDP-Im with pGL3-CV (pGL3 Alone), pGL3-CV and a control siRNA (pGL3+siCON1), or pGL3-CV and an siRNA against luciferase (pGL3+siLuc).

4.4.11 Nanoparticles are multifunctional, integrated systems for nucleic acid delivery

The results presented here highlight the importance of creating a nanoparticle that consists of multiple components that function together as a system, and control over size, surface modification, payload protection, and targeting ligand to payload ratio are key parameters to consider when designing nucleic acid delivery vehicles for in vivo systemic use. These parameters also represent some of the major advantages of nanoparticle composites for delivery of nucleic acids instead of using carrier-free delivery methods. Nucleic acid delivery vehicles can help reduce renal clearance while adding features such as stabilization against nuclease degradation, cell-specific targeting, and large payload

delivery. These features make them well-suited for the systemic delivery of nucleic acids in general, and we have shown that the system investigated here can deliver pDNA, siRNA, and DNAzymes in vitro and in vivo (7,17,19,20).

The capability to fine-tune the delivery vehicle's properties combined with an understanding of how those properties affect its function in biological systems represent two key factors necessary for optimization of nucleic acid delivery vehicles. This study demonstrates the importance of a rational approach in delivery vehicle design and lays a foundation for further in vivo studies to understand the relationships between the properties of nanoparticle delivery systems and their biological function. The approach to designing nanoparticle delivery vehicles that is outlined here can be used for other synthetic materials and is thus not limited to the cyclodextrin polymer-based system illustrated.

4.5 Acknowledgments

We thank Nicholas Brunelli (California Institute of Technology) for performing the atomic force microscopy imaging and Patrick Koen (California Institute of Technology) for performing the transmission electron microscopy imaging. D.W.B. acknowledges support from a National Science Foundation Graduate Research Fellowship. This publication was made possible by Grant Number 1 R01 EB004657-01 from the National Institutes of Health (NIH). Its contents are solely the responsibility of the authors and do not necessarily represent the official views of the NIH.

4.6 References

1. Morrissey, D.V., Blanchard, K., Shaw, L., Jensen, K., Lockridge, J.A., Dickinson, B., McSwiggen, J.A., Vargeese, C., Bowman, K., Shaffer, C.S. et al. (2005) Activity of stabilized short interfering RNA in a mouse model of hepatitis B virus replication. *Hepatology*, **41,** 1349-1356.
2. Layzer, J.M., McCaffrey, A.P., Tanner, A.K., Huang, Z., Kay, M.A. and Sullenger, B.A. (2004) In vivo activity of nuclease-resistant siRNAs. *RNA*, **10,** 766-771.
3. Schatzlein, A.G. (2003) Targeting of synthetic gene delivery systems. *J Biomed Biotechnol*, **2,** 149-158.
4. Soutschek, J., Akinc, A., Bramiage, B., Charisse, K., Constien, R., Donoghue, M., Elbashir, S., Geick, A., Hadwiger, P., Harborth, J. et al. (2004) Therapeutic silencing of an endogenous gene by systemic administration of modified siRNAs. *Nature*, **432,** 173-178.
5. Dykxhoorn, D.M., Palliser, D. and Lieberman, J. (2006) The silent treatment: siRNAs as small molecule drugs. *Gene Ther*, **13,** 541-552.
6. Song, E., Zhu, P., Lee, S.-K., Chowdhury, D., Kussman, S., Dykxhoorn, D.M., Feng, Y., Palliser, D., Weiner, D.B., Shankar, P. et al. (2005) Antibody mediated in vivo delivery of small interfering RNAs via cell-surface receptors. *Nat Biotechnol*, **23,** 709-717.
7. Hu-Lieskovan, S., Heidel, J.D., Bartlett, D.W., Davis, M.E. and Triche, T.J. (2005) Sequence-specific knockdown of EWS-FLI1 by targeted, nonviral delivery of small interfering RNA inhibits tumor growth in a murine model of Ewing's sarcoma. *Cancer Res*, **65,** 8984-8992.
8. Ogris, M., Brunner, S., Schuller, S., Kircheis, R. and Wagner, E. (1999) PEGylated DNA/transferrin-PEI complexes: reduced interaction with blood components, extended circulation in blood and potential for systemic gene delivery. *Gene Ther*, **6,** 595-605.
9. Morrissey, D.V., Lockridge, J.A., Shaw, L., Blanchard, K., Jensen, K., Breen, W., Hartsough, K., Machemer, L., Radka, S., Jadhav, V. et al. (2005) Potent and persistent in vivo anti-HBV activity of chemically modified siRNAs. *Nat Biotechnol*, **23,** 1002-1007.
10. Zimmermann, T.S., Lee, A.C.H., Akinc, A., Bramlage, B., Bumcrot, D., Fedoruk, M.N., Harborth, J., Heyes, J.A., Jeffs, L.B., John, M. et al. (2006) RNAi-mediated gene silencing in non-human primates. *Nature*, **441,** 111-114.
11. Plank, C., Mechtler, K., Szoka, F.C.J. and Wagner, E. (1996) Activation of the complement system by synthetic DNA complexes: a potential barrier for intravenous gene delivery. *Hum Gene Ther*, **7,** 1437-1446.
12. Chonn, A., Cullis, P.R. and Devine, D.V. (1991) The role of surface charge in the activation of the classical and alternative pathways of complement by liposomes. *J Immunol*, **146,** 4234-4241.
13. Venturoli, D. and Rippe, B. (2005) Ficoll and dextran vs. globular proteins as probes for testing glomerular permselectivity: effects of molecular size, shape, charge, and deformability. *Am J Physiol Renal Physiol*, **288,** F605-613.

14. Dreher, M.R., Liu, W., Michelich, C.R., Dewhirst, M.W., Yuan, F. and Chilkoti, A. (2006) Tumor vascular permeability, accumulation, and penetration of macromolecular drug carriers. *J Natl Cancer I*, **98,** 335-344.
15. Rensen, P., Sliedregt, L., Ferns, M., Kieviet, E., van Rossenberg, S., van Leeuwen, S., van Berkel, T. and Biessen, E. (2001) Determination of the upper size limit for uptake and processing of ligands by the asialoglycoprotein receptor on hepatocytes in vitro and in vivo. *J Biol Chem*, **276,** 37577-37584.
16. Mishra, S., Webster, P. and Davis, M.E. (2004) PEGylation significantly affects cellular uptake and intracellular trafficking of non-viral gene delivery particles. *Eur J Cell Biol*, **83,** 97-111.
17. Davis, M.E., Pun, S.H., Bellocq, N.C., Reineke, T.M., Popielarski, S.R., Mishra, S. and Heidel, J.D. (2004) Self-assembling nucleic acid delivery vehicles via linear, water-soluble cyclodextrin-containing polymers. *Curr Med Chem*, **11,** 1241-1253.
18. Mishra, S., Heidel, J.D., Webster, P. and Davis, M.E. (2006) Imidazole groups on a linear, cyclodextrin-containing polycation produce enhanced gene delivery via multiple processes. *J Control Release*, **116,** 179-191.
19. Bellocq, N.C., Pun, S.H., Jensen, G.S. and Davis, M.E. (2003) Transferrin-containing polymer-based particles for tumor-targeted gene delivery. *Bioconjugate Chem*, **14,** 1122-1132.
20. Pun, S.H., Bellocq, N.C., Cheng, J., Grubbs, B.H., Jensen, G.S., Davis, M.E., Tack, F., Brewster, M., Janicot, M., Janssens, B. et al. (2004) Targeted delivery of RNA-cleaving DNA enzyme (DNAzyme) to tumor tissue by transferrin-modified, cyclodextrin-based particles. *Cancer Biol Ther*, **3,** 31-40.
21. Blandamer, M.J., Cullis, P.M. and Engberts, J.B.F.N. (1998) Titration microcalorimetry. *J Chem Soc Faraday T*, **94,** 2261-2267.
22. Perry, C.S., Charman, S.A., Prankerd, R.J., Chiu, F.C.K., Scanlon, M.J., Chalmers, D. and Charman, W.N. (2006) The binding interaction of synthetic ozonide antimalarials with natural and modified β-cyclodextrins. *J Pharm Sci*, **95,** 146-158.
23. Hansen, P.L., Cohen, J.A., Podgornik, R. and Parsegian, V.A. (2003) Osmotic properties of poly(ethylene glycols): quantitative features of brush and bulk scaling laws. *Biophys J*, **84,** 350-355.
24. Pun, S.H. and Davis, M.E. (2002) Development of a nonviral gene delivery vehicle for systemic application. *Bioconjugate Chem*, **13,** 630-639.
25. Adams, G.P., Tai, M.-S., McCartney, J.E., Marks, J.D., Stafford III, W.F., Houston, L.L., Huston, J.S. and Weiner, L.M. (2006) Avidity-mediated enhancement of in vivo tumor targeting by single-chain Fv dimers. *Clin Cancer Res*, **12,** 1599-1605.
26. Phillips, J., Rutledge, L. and Winters, W. (1986) Transferrin binding to two human colon carcinoma cell lines: characterization and effect of 60 Hz electromagnetic fields. *Cancer Res*, **46,** 239-244.
27. Shir, A., Ogris, M., Wagner, E. and Levitzki, A. (2006) EGF receptor-targeted synthetic double-stranded RNA eliminates glioblastoma, breast cancer, and adenocarcinoma tumors in mice. *PLoS Med*, **3,** e6.